Mechanical characterization of visually graded boards from turkish fir and black pine by nondestructive and destructive tests

Fatih Kurul[1] https://orcid.org/0000-0002-4473-4159♣
Ömer Asım Şişman[2] https://orcid.org/0000-0001-9260-6402
Türker Dündar[1] https://orcid.org/0000-0002-3678-9993

[1]Istanbul University - Cerrahpaşa. Faculty of Forestry. Department of Wood Mechanics and Technology. İstanbul, Turkey.
[2]Gebze Technical University. Civil Engineering Faculty. Kocaeli, Turkey.

♣Corresponding author: fatihkurul@istanbul.edu.tr

Abstract:
For the mechanical characterization of Turkish fir and black pine, 400 board specimens with 22 mm× 50 mm × 420 mm were visually graded according to TS 1265 standard. Nondestructive tests were here upon performed using the stress wave method. After specimens were intentionally tested under flatwise bending to research the applicability as an alternative to tension and edgewise bending tests in European strength grading system. According to analyses of variance, the mean values of MOR and MOE differed in four groups at a $p<0,05$ significance level for visually graded boards. High correlations were found between MOR-MOE ($R^2=0,837$) for fir and MOR-MOE ($R^2=0,776$) for black pine. In addition, correlations of MOR-Knot rate for fir and black pine were respectively $R^2=0,669$ and $R^2=0,660$ showing the effectiveness of flatwise bending tests with the visual grading standard. For nondestructive tests, the mean values of the dynamic modulus of elasticity were very close in between fir and black pine grades while the usage of defect-free density performed better than the density of the whole specimen. Higher strength classes were found for black pine boards (Class 1= C40, Class 2= C27 and Class 3= C22) compared to fir boards (Class 1= C24, Class 2= C22 and Class 3= C18), respectively. Moreover, a simplified nonlinear material model was proposed for numerical modelling, and the results were found in good agreement in terms of the bending stiffness, strength, and deformation capacity of boards especially for class 1 and class 2 in both softwood species.

Keywords: Board, flatwise bending, finite element method, mechanical properties, stress wave, visual grading.

Introduction

Timber, as a natural and sustainable construction material, has variations in mechanical and physical properties due to anisotropy, defects and biological characteristics (Köhler *et al.* 2007). National standards such as DIN 4074-1 (2012), BS 4978: 2007+A2 (2017), UNI 11035-1 (2010) and UNE 56544 (2011) have been developed for visual grading of timber products based on knots, the slope of grain, strength, stiffness, density, and other visible parameters as described in EN 1912 (2012b). Timber products with a CE marking, representing the guaranteed resistance, are called strength graded timber that can be used to produce structural elements (Burawska-Kupniewska *et al.* 2020).

In addition to visual grading, nondestructive tests have been recently developed to evaluate the dynamic modulus of elasticity such as vibration, ultrasonic and stress wave methods and used in practice for an efficient grading of structural timber (Divós and Kiss 2010, Sanabria *et al.* 2011, Barriola *et al.* 2021).

Vibration method was prominent, however, the stress wave method was found to be more practical among nondestructive methods (Esteban *et al.* 2009, Barriola *et al.* 2020). Stress wave technique for wood quality assessment is based on the measurement of the velocity of a stress wave propagation generated by a shock. This technique is also applied for the production of engineered wood products (Bucur 2006, Ross 2015). According to Arriaga *et al.* (2022), velocities measured with the ultrasonic and stress wave methods had similar average value.

Moreover, the strength classes of structural timber are evaluated by machine grading that measure one or more mechanical and physical properties to establish its indicating properties (Mvolo *et al.* 2021, Vega *et al.* 2019). Kandler *et al.* (2018) experimentally tested glued laminated timber (GLT) beams to evaluate the impact of knots on bending strength and stiffness utilizing finite element model (FEM) with the image-processing.

For cross-laminated timber (CLT) panels produced from Australian pine, Navaratnam *et al.* (2020) predicted bending and shear performance using FEM analysis which was validated by experimental test data. Pang *et al.* (2021) investigated the effects of knots on the flexural performance of CLT panels to enhance the potential of using low-grade boards.

Furthermore, Crovella *et al.* (2019) verified shear analogy approach to evaluate bending stiffness of CLT panels made from softwood and hardwood. Rais *et al.* (2021) investigated European beach boards using 3D fiber orientation via laser technique for tensile strength prediction. The shift from structural timber to engineered wood products such as GLT post & beam and CLT wall or floor panels increased the speed and height of timber structures.

In recent years, the use of visual grading has gained momentum in Turkey for sustainable development and constructing timber buildings using green-certified products. Görgün and Dündar (2018) examined the compatibility between visual grades and the mechanical properties of timber joists from Turkish black pine determined by using nondestructive methods and edgewise bending tests. Moreover, Guntekin and Bulbul (2014) and Guntekin *et al.* (2013) used the stress wave method for the determination of the mechanical properties of timber joists from Turkish black and red pine, respectively.

Black pine is the second most common pine species following Turkish red pine, constituting 31 % of the softwood forest corresponding to 19 % of the total forestland in Turkey (OGM 2021). On the other hand, fir forest constitutes 3 % of the forestland in Turkey. Both species are also regarded as raw materials with a high potential for engineered wood products for structural usage in the timber industry.

Before the lamination process, boards shall be strength graded and declared as tabulated strength class in accordance with EN 14080 (2013) for GLT and EN 16351 (2015) for CLT. The entire system of strength grading and loading protocols in Europe are focused in edgewise bending or tension tests although boards used in engineered wood products are stressed in

flatwise bending (Stapel and van de Kuilen 2014). This implies the need for research to verify the applicability of flatwise bending testing for the European standardization with C classes.

The motivation of this study was to determine the mechanical characterization of visually graded boards using flatwise bending tests to check whether the strength classes in EN 338 (2016b) obtained by edgewise bending tests are similar for Turkish fir and black pine timber. For the nondestructive testing, the stress wave method is investigated to evaluate the potential applicability and effectiveness for grading. Furthermore, a simplified nonlinear material model was proposed for the numerical modelling of boards in structural applications like flooring or a layer definition of CLT panels and GLT beams.

Materials and methods

In this study, flatwise bending tests are arranged for 400 specimens with 22 mm ×50 mm ×420 mm (depth·with ·length of boards) including 200 fir (*Abies nordmanniana* subsp. *Bornmuelleriana)* from Bolu region and 200 black pine (*Pinus nigra Arnold. subsp. pallasiana*) from Balıkesir region from Turkey as described in Table 1. The length of specimens is selected as 19 times the depth of boards, which is shorter than edgewise bending tests. The moisture contents of boards were measured using the oven dry method by following the procedure defined in EN 13183-1 (2002). The average moisture contents were found as 11,4 % both fir and black pine.

Table 1: Sample distribution for fir and black pine boards.

Species	Dimensions (mm)	Visual grade	Specimens	Moisture Content
Fir	22 ×50 ×420	1	50	11,4 %
		2	50	
		3	50	
		Rejected	50	
Black Pine		1	50	11,4 %
		2	50	
		3	50	
		Rejected	50	

In the outline of the research, specimens are first visually sorted as shown in Figure 1. Then, boards are tested by the stress wave method due to its easy applicability and the lack of experimental data in the literature. Next, boards are destructed using a flat wise bending test setup. Afterwards, a numerical model is proposed. Finally, the destructive and nondestructive results are analyzed statically for the comparison and discussed in detail.
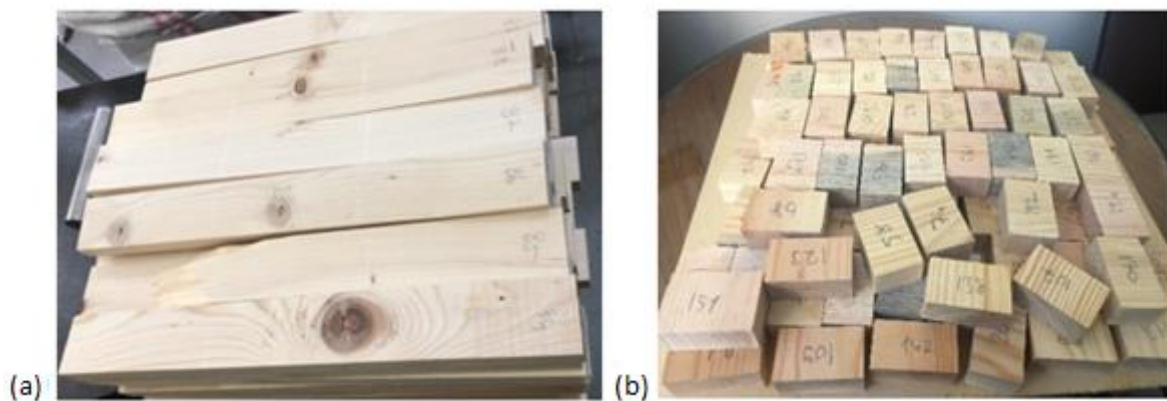

Figure 1: Visually graded (a) board specimens with defects and (b) defect-free cut fir and black pine pieces after the tests.

Visual grading

All specimens used in this study were classified according to TS 1265 (2012). For structural usage, softwood timber products were sorted into three grades: class 1 with high load-bearing capacity, class 2 with moderate load-bearing capacity, and class 3 with low load-bearing capacity. On the other hand, the boards that did not match any of the grading requirements were referred to as rejected. Although the knot area ratio (KAR) is used for visual grading before the lamination process in the standard of ASTM D3737 (2018), TS 1265 (2012) requires calculating the knot diameter ratio (KDR) for each board specimen. KDR is defined as the knot diameters divided by twice the width of the board. Therefore, knot dimensions were visually checked and measured through the length of specimens. As shown in Figure 2a, knot diameter is measured by the surface which is parallel to the board. Moreover, the knot clusters are calculated by the sum of the KDRs of the knots existing in any 150 mm length of a piece of boards as shown in Figure 2b. Visual grading criteria for structural timber boards were defined in Table 2 according to TS 1265 (2012).
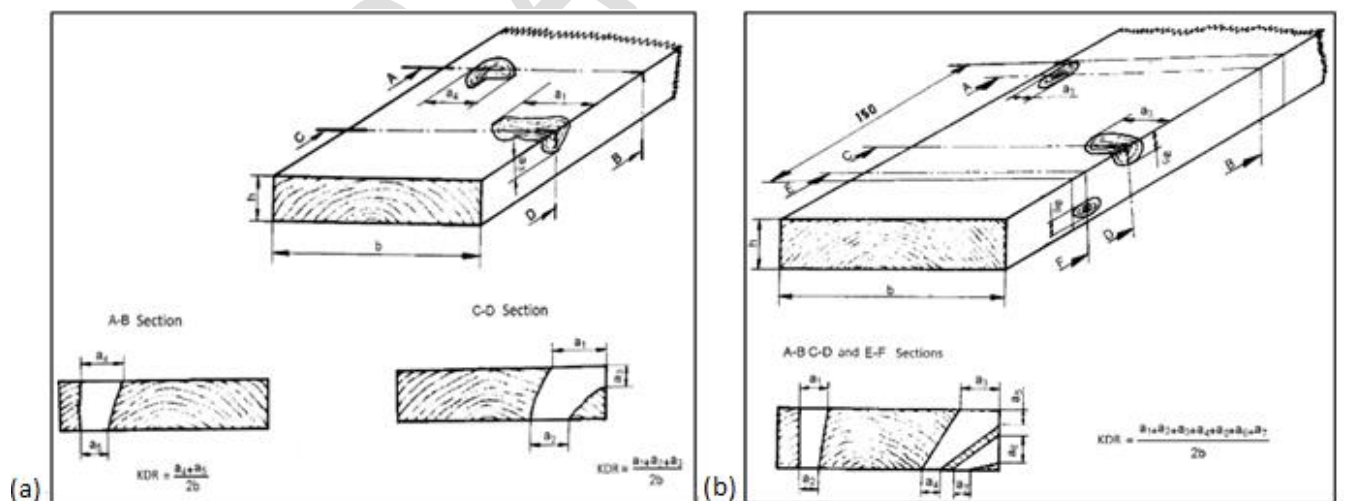

Figure 2: (a) Measurement method of single knots, (b) Measurement method of knot clusters (for boards according to TS 1265 (2012).

Moreover, the slope of grain, annual ring width and other defects were measured as specified in EN 1309-3 (2018b). Then, all specimens were cut according to the location of critical knots

to be placed in between the loading points. Apart from visual grading, the angle between the flat surface of the samples and annual rings, αwas also measured for each specimen. Then, specimens were grouped as 0°-30° (tangential),30°-60° (rift) and 60°-90° (radial) as shown in Figure 3 according to EN 844 (2019).

Table 2: Visual grading of structural timber boards according to TS 1265 (2012).

| Characteristics	Grades		
	Class 1	Class 2	Class 3
Knot The ratio of the sum of the knot dimensions on each face to twice the width of the piece	1/5	1/3	1/2
Knot cluster The ratio of the sum of the knot dimensionsmeasured perpendicular to the timber axis, within the worst 150 mm length, to twice the width	1/3	1/2	2/3
Slope of grain	Deviation in 1 mlength is not greater than:		
a) In case of presence of surface fissure b) In case of no surface fissure	70 mm 100 mm	120 mm 200 mm	200 mm 300 mm
Annual ring width	Growth ring area bigger than 4 mm should not be greater than 1/2 of the whole cross-section	No limitation	No limitation
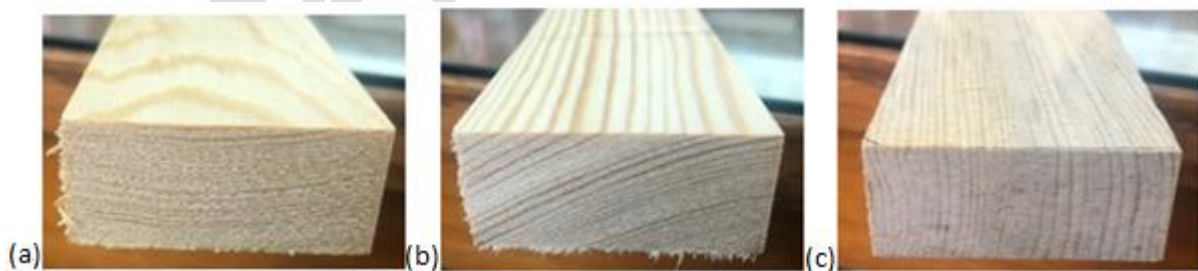
Figure 3: Angle between the flat surface of the samples and annual ring, α: (a) 0°-30°(tangential) (b) 30°-60° (rift) and (c) 60°-90° (radial).

Nondestructive test method

Following the visual grading, the dynamic modulus of elasticity (MOEd) was determined for each specimen by using stress wave method with a portable microsecond stress wave timer. Fakopp Microsecond Timer (23 kHz) has two piezoelectric-type transducers with 60 mm long spikes as shown in Figure 4. For the application, the source is selected as a simple hammer impact and then the time of flight is measured. Then, stress wave velocity (m/s) was calculated using the distance between the transducers (L, m) and the time of flight taken from the device (Δt, μs) by the following equation (Equation 1). After that, dynamic modulus of elasticity was calculated with two different methods. $MOEd_1$ (MPa) included the whole specimen's density (ρ_1, kg/m^3) as a standard method but the density of defect-free piece was proposed by $MOEd_2$ (MPa) which is cut from the same specimen (ρ_2, kg/m^3) by the following equations (Equation 2 and Equation 3). Meanwhile, whole specimens' density (ρ_1) was calculated by volume and mass however defect-free density (ρ_2) was calculated after the destructive tests.

Figure 4: Measuring time of flight with Fakopp micro seccond timer.

$$V = \frac{L}{\Delta t} \qquad (1)$$

$$MOEd_1 = V^2 \rho_1 \qquad (2)$$

$$MOEd_2 = V^2\rho_2 \qquad (3)$$

Destructive test method

After the nondestructive tests, 400 boards with 22 mm $\times$50 mm $\times$420 mm were tested flatwise

in a four-point bending test setup as stipulated in EN 408 (2012a) with a 396 mm span length.

Tests were carried out with the universal testing machine, which was equipped with a load cell

of 100 kN. All specimens were tested under flatwise bending, and the deformations (w) were

measured at the center of the span. Thereby, global modulus of elasticity (MOE) and modulus

of rupture (MOR) were determined by following Equation 4 and Equation 5.

$$MOE = \frac{3al^2 - 4a^3}{2bh^3\left(2\dfrac{w_2 - w_1}{F_2 - F_1} - \dfrac{6a}{5Gbh}\right)} \qquad (4)$$

$$MOR = \frac{3F_{max}a}{bh^2} \qquad (5)$$

Where: MOE is the global modulus of elasticity (MPa), MOR is the modulus of rupture (MPa),

l is the span distance (mm), a is the distance between a loading position and the nearest support

in a bending test (mm), F_2-F_1 is the load difference at 10 % and 40 % of maximum load (N),

w_2-w_1 is the deflection difference at 10 % and 40 % of maximum load (mm), G is the shear

modulus assumed as 650 MPa, b is the with (mm) and h is the height of samples (mm). The

defect-free density (d_2) of each specimen at the moisture content during the test was determined

from a piece of the board cut as close as the location of the fracture after the experiments. Then, the pieces were immediately weighed with an accuracy of 0,01 g and their dimensions were measured with an accuracy of 0,01 mm. Furthermore, the moisture contents were found with the same samples by following the procedure defined in EN 13183-1 (2002).

Characteristic value

According to EN 384 (2018a), there are several adjustments required for obtaining characteristic values:

The experimental values for the modulus of elasticity and the density of specimens that were not at the reference moisture content, were adjusted by using the following formulas (Equation 6 and Equation 7):

$$MOE_{(12\%)} = MOE(u)\left(1 + 0,01(u - u_{ref})\right) \qquad (6)$$

$$d_{2(12\%)} = d_2(u)\left(1 - 0,005(u - u_{ref})\right) \qquad (7)$$

Where: u is the moisture content at testing (8 % ≤ u ≤ 18 %), and u_{ref} is the reference moisture content (normally u_{ref} = 12 %).

MOR shall be adjusted to 150 mm depth by dividing with the factor k_h as described in the formula. Therefore, the bending strength values obtained from the samples with a depth of nominal 22 mm were adjusted to 150 mm depth by dividing by the factor k_h (Equation 8).

$$k_h = Min \left\{ \left(\frac{150}{h} \right)^{0,2} \atop 1,3 \right. \qquad (8)$$

MOE shall be adjusted to the modulus of elasticity E_0 by using the following formula (Equation 9):

$$E_0 = MOE_{(12\%)} 1,3 - 2690 \qquad (9)$$

After completing the required adjustments, the 5-percentile strength values $f_{05,i}$, defect-free density $d_{05,i}$ and the mean stiffness values were determined for each grade of fir and black pine species as stimulated in EN 14358 (2016a) where bending strength and density were assumed as logarithmically distributed and modulus of elasticity was assumed as normally distributed. Thus, the parametric method was used to calculate the 5-percentile values of bending strength and density. The coefficient of subsample was neglected because specimens were delivered from one region only.

Numerical modelling

Numerical studies focused previously on the mechanical characterization of timber such as bending strength and stiffness (Berg *et al.* 2019, Olsson *et al.* 2013), tensile strength and stiffness (Mitsuhashi *et al.* 2008, Kohler *et al.* 2013). In this study, a simplified nonlinear material model was adopted to capture both elastic and plastic zones for modelling the out-of-

plane bending behavior of boards in structural applications. Hence, the material models of fir and black pine species were generated for each grade using the stress distribution as shown in Figure 5. The distinct characters of tension parallel-to-grain and compression parallel-to-grain of timber under bending were expressed separately in the material model. For each visual grade, ultimate tension stress ($f_{t,0,u}$) of boards was taken as equal to the mean values of ultimate bending stress f_m according to Nwokoye (1972). Bending behavior of boards in tension stress was defined as linear brittle material where the mean values of the elastic modulus E_{mean} were obtained from the experimental tests. However, bending behavior in compression stress was defined as ideal elasto-plastic material using E_{mean} and the ultimate stress of compression parallel-to-grain ($f_{c,0,u}$) was assumed to be reached at 0,003 mm/mm based on (Frese *et al.* 2012). In the numerical models, the support conditions of a simple beam and vertical loads according to four-point bending were firstly defined in SAP 2000 software (2000) as described in the test setup as shown in Figure 6. Then, boards were created using 2D layered/nonlinear shell elements with the simplified nonlinear material models for each grade and species. Finally, the vertical loads were increased step by step to find out peak displacements and load-carrying capacities of boards under bending. The tensile and compressive stress distributions can be also seen in Figure 6.
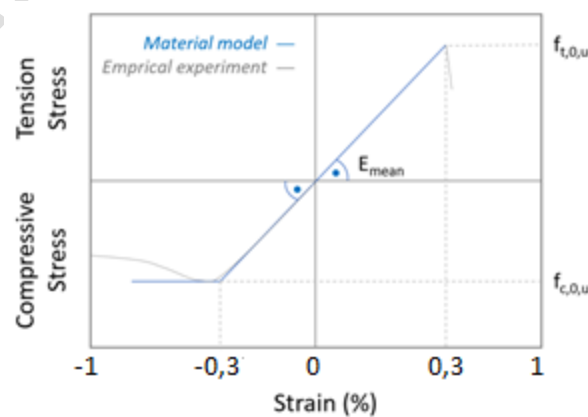

Figure 5: Simplified nonlinear material model for boards under bending.
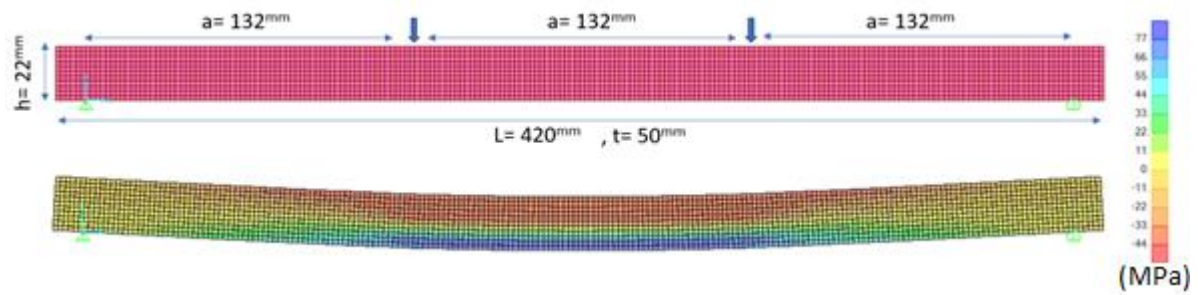
Figure 6: Numerical model and the stress distribution of a board under bending.

Results and discussions

The destructive and nondestructive results were used for the analysis of variance (ANOVA) to detect whether any significant differences exist statistically within density values, MOR, MOE, velocity, $MOEd_1$ and $MOEd_2$ considering the visual grades of the specimens based on TS 1265 (2012). Average values for moisture content, ρ_1, ρ_2, MOR, MOE, velocity and $MOEd_1$ and $MOEd_2$ were given separately for each visual grade in Table 3 and Table 4, for fir and black pine species respectively.

Furthermore, the standard deviation values were given in parentheses. Afterwards, Duncan test was applied to the variables that had significant differences and grouped as shown with lower-case letters over the mean values.

Table 3: Nondestructive and destructive test results and ANOVA for fir.

Fir / Grade	N	Moisture Content (%)	ρ_1(kg/m³)	ρ_2(kg/m³)	MOE (MPa)	MOR (MPa)	Velocity (m/s)	MOEd$_1$ (MPa)	MOEd$_2$ (MPa)
Class 1	50	11,3 (0,6)	418[a] (37,7)	412[a] (33,5)	12176,9[a] (1885,6)	67,0[a] (9,9)	4837,0[a] (223,0)	9809,5[a] (1322,1)	9656,3[a] (1364,3)
Class 2	50	11,5 (0,6)	425[ab](37,3)	410[a] (39,4)	10530,0[b] (1369,7)	52,5[b] (9,2)	4663,9[b] (204,2)	9257,7[b] (1113,7)	8895,8[b] (1073,6)
Class 3	50	11,4 (0,5)	437[b] (38,0)	409[a] (32,1)	9323,8[c] (1224,8)	43,7[c] (8,3)	4592,5[b] (219,6)	9222,7[b] (1029,1)	8605,6[b] (1047,6)
Rejected	50	11,3 (0,4)	462[c] (37,4)	411[a] (23,9)	6383,6[d] (1818,1)	25,8[d] (8,8)	4388,3[c] (254,6)	8922,0[b] (1025,0)	7907,0[c] (996,0)

( ): standard deviation.
Different letters show that there is a difference for each test value (p<0,05)

Table 4: Nondestructive and destructive test results and ANOVA for black pine.

Black Pine/ Grade	N	Moisture Content (%)	ρ_1(kg/m³)	ρ_2(kg/m³)	MOE (MPa)	MOR (MPa)	Velociy (m/s)	MOEd$_1$ (MPa)	MOEd$_2$ (MPa)
Class 1	50	11,7 (0,9)	512[a] (55,7)	507,0[a] (59,4)	13578,0[a] (2509,0)	77,5[a] (12,7)	4693,0[a] (188,5)	11339,2[a] (1844,7)	11211,1[a] (1840,8)
Class 2	50	11,3 (0,8)	519[a] (56,1)	502,0[a] (52,3)	11515,5[b] (2276,2)	61,7[b] (12,4)	4518,1[b] (268,2)	10661,7[ab] (1914,5)	10288,5[b] (1911,3)
Class 3	50	11,3 (1,0)	516[a] (56,3)	492,0[a] (47,3)	10053,1[c] (2072,4)	52,1[c] (11,9)	4406,2[b] (315,0)	10094,1[b] (1835,5)	9602,4[bc] (1855,1)
Rejected	50	11,2 (0,8)	546[b] (56,1)	493,3[a] (52,3)	7876,0[d] (2282,8)	32,0[d] (12,0)	4231,2[c] (378,5)	9906,6[b] (2264,3)	8951,3[c] (2165,7)

( ): standard deviation.
Different letters show that there is a difference for each test value (p<0,05)

In the visual grades, ANOVA was performed for each variable to determine whether there was any difference as equal to a significance level of p<0,05. According to Table 3 and Table 4, a significant difference was not found in ρ_2 as expected for the defect-free pieces compared to $\rho_1$for fir and black pine species, respectively. However, significant differences were found in MOR and MOE. For both species, the mean values of MOR and MOE decreased in lower visual classes as it was anticipated for visual grading.

Using stress wave method, three groups were found between velocity values as class 1, class 2-3 and rejected for both species. Due to the location and large size of edge knots as shown in Figure 7, the prediction of velocity varied significantly in board specimens other than class 1 that may lead to unconservative results. According to mean values of MOE, class 1 and 2 were higher than mean values of dynamic modulus of elasticity but class 3 was almost equal for both species.

In the studies of Van Duong and Matsumura (2018) and Van Duong and Ridley-Ellis (2021), however, the modulus of elasticity values obtained by three-point bending tests were about 15 % lower than the dynamic modulus of elasticity values measured by the stress wave method for small clear wood samples with 20 mm ×20 mm ×320 mm length. The difference between MOE and MOEd could be attributed to tested specimens with defects and the four-point bending test setup used in this paper.

Figure 7: Knot locations (a) at the wide face (b) big knot and (c) small knot at the narrow face.

For each visual grade, the difference between $MOEd_1$ and $MOEd_2$ was resulted from the density of the defect-free pieces. The mean values of $MOEd_1$ were higher than the mean values of $MOEd_2$ which was caused by the increased weight with higher density of knots especially for class 3 and rejected samples. Hence, $MOEd_2$ groups went parallel with velocity remarkably for fir and black pine and more effective to detect rejected samples. For fir, the ratios between MOE and $MOEd_2$ were 0,79 for class 1; 0,85 for class 2; 0,92 for class 3 and 1,24 rejected samples, respectively.

On the other hand, the ratios between $MOEd_1$ and MOE were 0,81 for class 1; 0,88 for class 2;0,99 for class 3 and 1,39 for rejected specimens in fir, respectively. In black pine, the ratios between $MOEd_2$ and MOE were 0,82 for class 1; 0,89 for class 2; 0,96 for class 3 and 1,14 for rejected samples, respectively where the ratios between MOE and $MOEd_1$ were 0,84 for class 1; 0,93 for class 2 and 1,01 for class 3 and for 1,26 rejected samples, respectively. Please note

that $MOEd_1$ and $MOEd_2$ overestimated the modulus of elasticity of rejected samples while defect-free density performed better compared to whole specimens' density.

In addition, no significant difference was found for the angle, α in destructive and nondestructive results according to Duncan tests according to Table 5. Therefore, the mechanical properties of boards were not affected remarkably by the angle, α under bending.

Table 5: ANOVA for the angle, α in destructive and nondestructive results.

Species	α	N	MOE (MPa)	MOR (MPa)	Velocity (m/s)	$MOEd_1$ (MPa)	$MOEd_2$ (MPa)
			Subset for alpha = 0,05				
Fir	0°-30°	102	9993,2[a]	49,6[a]	4629,1[a]	9393,9[a]	8874,2[a]
	30°-60°	64	9174,7[a]	43,5[a]	4601,2[a]	9138,9[a]	8564,6[a]
	60°-90°	34	9241,9[a]	47,5[a]	4630,7[a]	9339,3[a]	8821,6[a]
	Sig.		0,127	0,085	0,604	0,285	0,238
Black Pine	0°-30°	91	10664,0[a]	53,9[a]	4446,8[a]	10524,1[a]	9867,8[a]
	30°-60°	74	10966,9[a]	57,7[a]	4465,3[a]	10556,4[a]	10113,8[a]
	60°-90°	35	10547,3[a]	56,6[a]	4479,5[a]	10320,2[a]	9867,8[a]
	Sig.		0,502	0,365	0,634	0,567	0,565

Different letters show that there is a difference for each test value (p<0,05)

Regression and correlation matrices

The frequency histograms of specimens and regression matrix of mechanical properties were plotted using MOR-MOE, MOR-knot rate, MOE-knot rate, MOR-velocity, MOE-velocity and knot rate-velocity. Linear regression matrices for MOR, MOE, knot rate and velocity were shown in Figure 8 and Figure 9 for fir and black pine respectively. In the matrix, histograms were located at the points where the variables coincided with each other. For fir, there were very strong correlations in MOR-MOE (R^2=0,837), MOR-Knot rate (R^2=0,669) and MOE-Knot rate (R^2=0,616).

Furthermore, strong correlations were found in MOR-Velocity (R^2=0,430), MOE-Velocity (R^2=0,554) and a moderate correlation was found in Velocity-Knot rate (R^2=0,307). For black pine, there were very strong correlations in MOR-MOE (R^2=0,776), MOR-Knot rate (R^2=0,660) and MOE-Velocity (R^2=0,700). Similarly, strong correlations were found in MOR - Velocity (R^2=0,489) and MOE-Knot rate (R^2=0,474). In addition, there was a moderate correlation in Velocity-Knot rate (R^2=0,253). For clarity and better understanding, the relations of $MOEd_1$ and $MOEd_2$ were presented separately using correlation matrix.
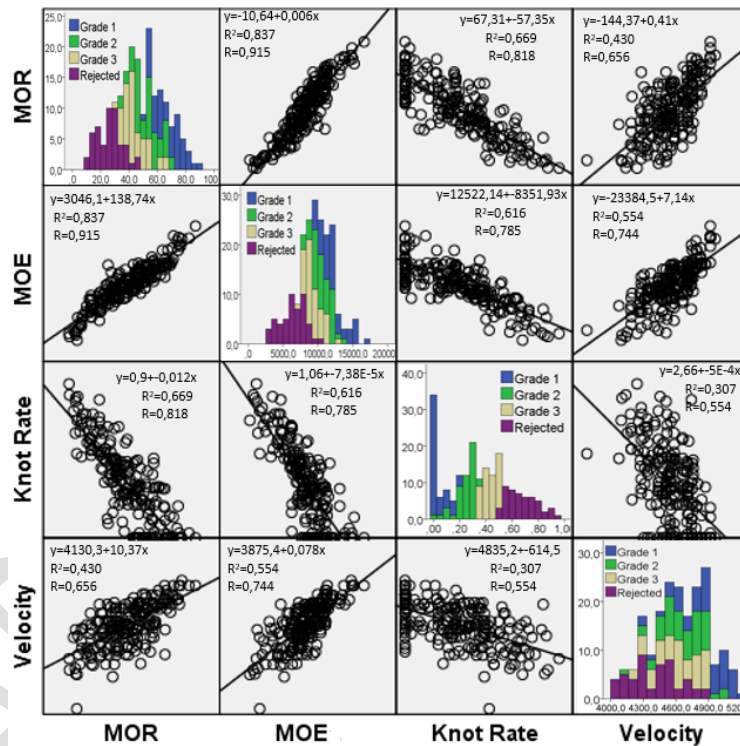

Figure 8: Regression matrix of MOR, MOE, knot rate and velocity for fir.
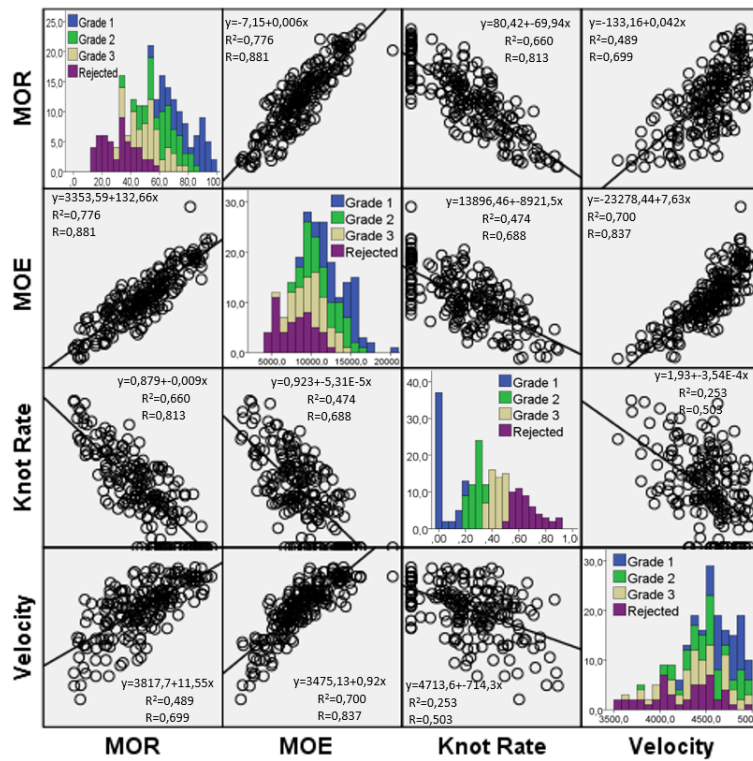
Figure 9: Regression matrix of MOR, MOE, knot rate and velocity for black pine.

For sub-groups of visual grading, correlation matrices for MOR, MOE, knot rate and velocity as well as $MOEd_1$ and $MOEd_2$ were given in Table 6 and Table 7 for fir and black pine, respectively. For fir specimens, Table 6 shows that by using proposed defect-free density instead of the density of whole specimen, the overall correlations of MOR-$MOEd_2$ and MOE-$MOEd_2$ increased by 90 % and 56 % compared to MOR-$MOEd_1$ and MOE-$MOEd_1$, respectively. Likewise, the overall correlations of MOR-$MOEd_2$ and MOE-$MOEd_2$ increased by 46 % and 19 % compared to $MOEd_1$ for black pine, respectively. More over, the overall correlation of velocity-$MOEd_2$ increased by 25 % for fir and 9 % for black pine compared to $MOEd_1$, respectively.

Table 6: Correlation matrix for sub-groups of fir.

Visual grade		MOR	MOE	Knot Rate	Velocity	MOEd$_1$	MOEd$_2$
1		-	0,720	0,016	0,342	0,609	0,595
2		-	0,380	0,145	0,045	0,160	0,172
3	MOR	-	0,412	0,000	0,115	0,168	0,235
Rej.		-	0,704	0,230	0,114	0,107	0,125
Overall Cor.		-	0,837	0,669	0,430	0,227	0,432
1		-	-	0,003	0,508	0,855	0,857
2		-	-	0,124	0,256	0,632	0,629
3	MOE	-	-	0,038	0,378	0,476	0,544
Rej.		-	-	0,333	0,239	0,172	0,206
Overall Cor.		-	-	0,616	0,554	0,379	0,592
1		-	-	-	0,023	0,041	0,024
2		-	-	-	0,000	0,231	0,161
3	Knot Rate	-	-	-	0,005	0,033	0,018
Rej.		-	-	-	0,007	0,002	0,000
Overall Cor.		-	-	-	0,307	0,034	0,176
1		-	-	-	-	0,657	0,680
2		-	-	-	-	0,341	0,381
3	Velocity	-	-	-	-	0,550	0,559
Rej.		-	-	-	-	0,793	0,795
Overall Cor.		-	-	-	-	0,555	0,686

Table 7: Correlation matrix for sub-groups of black pine.

Visual grade		MOR	MOE	Knot Rate	Velocity	MOEd$_1$	MOEd$_2$
1	MOR	-	0,627	0,071	0,401	0,525	0,546
2		-	0,709	0,000	0,468	0,523	0,518
3		-	0,429	0,015	0,169	0,201	0,232
Rej.		-	0,625	0,351	0,470	0,238	0,353
Overall Cor.		-	0,776	0,660	0,489	0,299	0,436
1	MOE	-	-	0,056	0,525	0,793	0,783
2		-	-	0,000	0,653	0,843	0,820
3		-	-	0,102	0,671	0,740	0,748
Rej.		-	-	0,235	0,754	0,666	0,768
Overall Cor.		-	-	0,474	0,700	0,626	0,743
1	Knot Rate	-	-	-	0,000	0,002	0,004
2		-	-	-	0,000	0,008	0,008
3		-	-	-	0,151	0,173	0,185
Rej.		-	-	-	0,135	0,037	0,067
Overall Cor.		-	-	-	0,253	0,067	0,152
1	Velocity	-	-	-	-	0,563	0,565
2		-	-	-	-	0,701	0,684
3		-	-	-	-	0,778	0,769
Rej.		-	-	-	-	0,807	0,871
Overall Cor.		-	-	-	-	0,700	0,765

Strength classes of fir and black pine

The strength class CXX defines the bending strength of edgewise bended samples in the strength grading of Europe whereas specimens were intentionally tested flat wise in this paper to research the potential for the applicability. After the 5 % percentile values of bending strength, modulus of elasticity and density were calculated, strength classes were declared in accordance with CEN EN 338 (2016b) for fir in Table 8 and black pine in Table 9.

Although the characteristic bending strength of fir and black pine were respectively determined as 39 MPa and 43,2 MPa in class 1, lower strength classes are attained due to the low density and modulus of elasticity for both species: C24 for fir and C40 for black pine. Similarly, boards

with class 2 were attained as C22 and C27 whereas class 3 boards were attained as C18 and C22 for fir and black pine, respectively. On the other hand, rejected grades could not be included in any strength class due to the limited capacity of bending strength and modulus of elasticity for both species.

To compare the strength classes obtained by flatwise bending with edgewise bending, Anatolian black pine and Caucasian and taurus fir species of Turkey presented in CEN EN 1912 (2012b) were used. Higher resistances were found for black pine boards (Class 1= C40, Class 2= C27 and Class 3= C22) in flatwise bending tests compared to strength classes using edgewise bending tests where Class 1= C35, Class 2= C24 and Class 3= C18. Similarly, same resistances were found for fir boards in Class 1= C24 and Class 3= C18 however a small decrease is found for Class 2 as equal to C22 in flatwise bending compared to C24 in edgewise bending tests.

Table 8: Determination of strength classes for fir.

0,05 Value per Class for Fir		Moisture Content at Testing (%)		Adjusted Bending Strength (MPa)				Adjusted Modulus of Elasticity (GPa)		Adjusted Density (kg/m³)			Strength Class
Class	No of Pieces	Mean	CoV	Mean	CoV	P/ NP	$f_{05,i}$	$E_{0,mean}$	CoV	Mean	CoV	$\rho_{05,i}$	
1	50	11,3	5,0	51,6	14,8	P	39	12,9	18,6	412,4	8,1	354,9	C24
2	50	11,5	5,4	40,4	17,6	P	28,7	10,9	16,2	409,8	9,6	341,5	C22
3	50	11,4	4,2	33,6	19,0	P	23,7	9,3	16,9	408,6	7,9	354,0	C18
Rej.	50	11,3	4,2	19,9	34,0	P	9,8	5,0	42,1	410,7	5,8	368,9	-

Table 9: Determination of strength classes for black pine.

0,05 Value per Class for Black Pine		Moisture Content at Testing (%)		Adjusted Bending Strength (MPa)				Adjusted Modulus of Elasticity (GPa)		Adjusted Density (kg/m³)			Strength Class
Class	No of Pieces	Mean	CoV	Mean	CoV	P/ NP	$f_{05,i}$	$E_{0,mean}$	CoV	Mean	CoV	$\rho_{05,i}$	
1	50	11,7	7,7	59,58	16,4	P	43,2	14,6	21,8	507,0	11,7	407,0	C40
2	50	11,3	6,8	47,42	20,1	P	31,4	11,9	24,1	501,9	10,4	415,2	C27
3	50	11,3	8,6	40,07	22,8	P	25,3	10,0	26,0	492,0	9,6	410,6	C22
Rej.	50	11,2	7,0	24,62	37,5	P	11,0	6,9	39,3	493,3	10,6	400,2	-

Failure modes and load-deflection relationships

The failure mode of boards can be summarized generally in three stages: (I) the stresses of beam section were in the linear elastic zone with low deflections on the middle span, and (II) linear elastic point was exceeded in the load-deflection curve and plastic deformations increased with the compression strains started to accumulate in the upper side of the board close to the loading head, then (III) the ultimate deflection was reached with brittle tension rupture of timber grains at the bottom of the board due to high tensile demands under bending as shown in Figure 10. However, the tension rupture of timber grains occurred earlier in grades with high KDR values. Therefore, the second stage was developed rapidly with very limited plasticity in class 3 and rejected specimens. For instance, the mean ultimate deformation capacity of boards in rejected class was found lower than other strength classes for both species.

In addition, the transition point that defines the start of plastic region and softening was found for each specimen by monitoring the change in the slope of the load-deflection curves with a correlation coefficient of 0,99 after exceeding linear load limit beyond 40 % of the peak load. The mean values of force, F_t and deflection, D_t were given in Table10 at the transition point for fir and black pine grades. While class number gets better, the mean values of force and deformation were increased in both species.

Figure 10: Brittle tension rupture of structural timber board.

Table 10: Transition points for fir and black pine grades.

Species	Fir		Black Pine	
Visual Grades	F_t(kN)	D_t(mm)	F_t(kN)	D_t(mm)
Class 1	1,81	4,18	2,11	4,33
Class 2	1,47	3,79	1,74	4,17
Class 3	1,25	3,61	1,43	3,93
Rejected	0,72	3,06	0,89	3,11

The experimental load-deflection curves of specimens were displayed for fir and black pine species respectively in Figure 11 and Figure 12 with the numerical models generated for each visual grade. From the comparison of load-deformation curves and numerical models, the simplified nonlinear material model was able to capture sufficiently not only the linear behavior but also the plastic behavior with a sudden drop in strength after the tensile rupture of timber parallel-to-grain under bending.

After the experimental tests, the mean values of the ultimate deflection, $D_{max,m}$ at the mid-span when 80 % of the ultimate load was reached at the descending part of the load-deformation curve and the mean values of the ultimate load, $F_{max,m}$ obtained in tests were also calculated and given in Table 11 for fir and black pine visual grades to compare the accuracy of the numerical modelling. Table 11 illustrates that the numerical model estimated the bending strength

accurately with a difference of 0,24 % and 2,77 % respectively for class 1 and class 2 but higher differences were found for class 3 and rejected for fir grades.

In black pine grades, the numerical model caught the bending strength with a maximum difference of 3,97 % in visual classes except for the rejected specimens. Although the deformation capacities were estimated with high accuracy for class 1 and class 2, the simplified material model overestimated deformation capacities of the class 3 for both species. As a result of the high KDR values, the failure mode tended to be more brittle compared to specimens with fewer defects leading unconservative deflection results in class 3. Finally, the proposed material model should not be utilized for the rejected specimens which are forbidden to be used in structural elements.
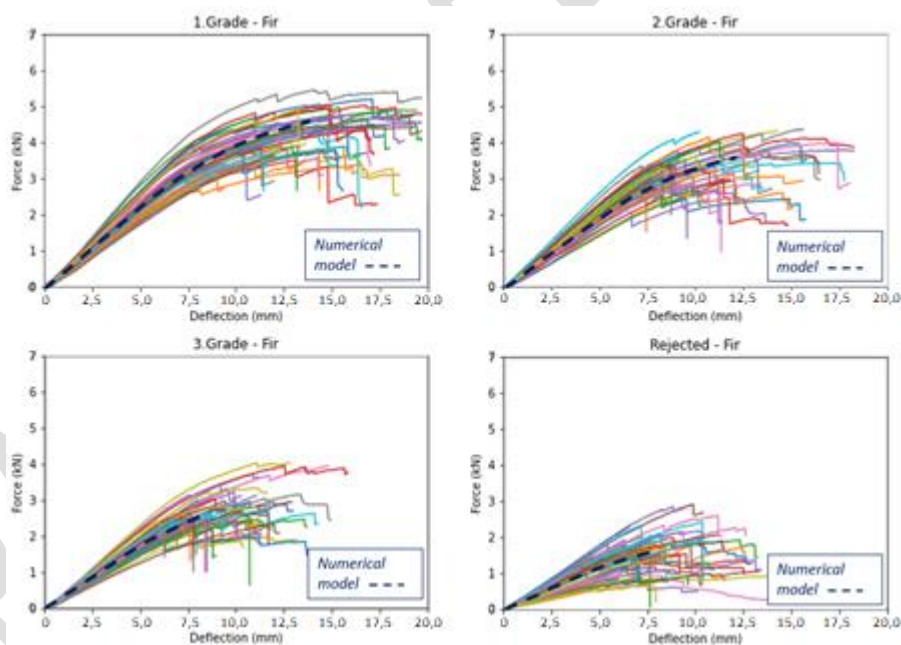

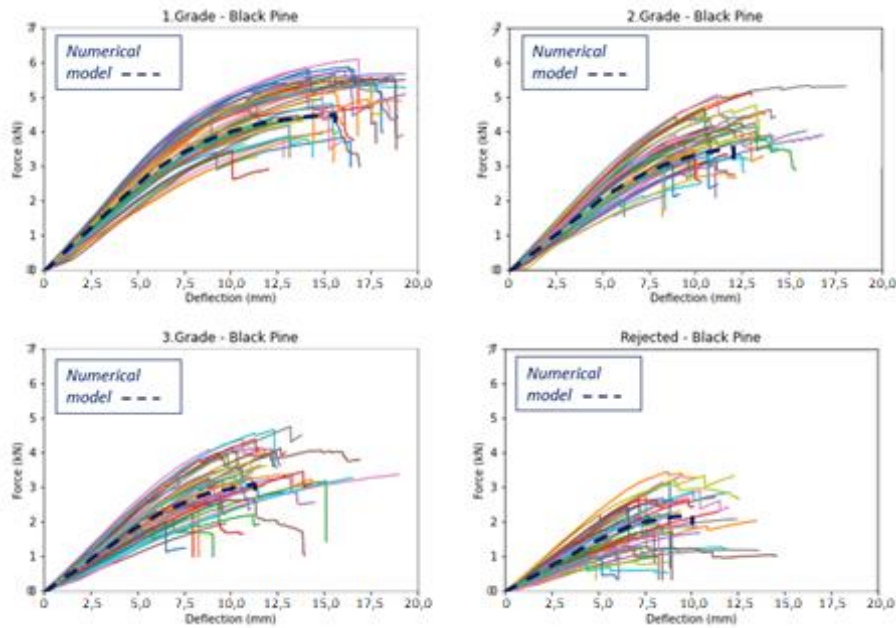**Figure 11:** Load and deflection relationship of fir grades.

Figure 12: Load and deflection relationship of black pine grades.

Table 11: Comparison of test and numerical results for fir and black pine grades.

Species		Fir		Black Pine	
Visual Grades		$F_{max,m}$ (kN)	$D_{max,m}$ (mm)	$F_{max,m}$ (kN)	$D_{max,m}$ (mm)
Class 1	Test	4,14	15,34	4,79	15,37
	Model	4,15	15,39	4,60	14,47
	Difference	0,24%	0,33%	-3,97%	-5,86%
Class 2	Test	3,25	11,88	3,78	11,76
	Model	3,34	12,04	3,74	11,98
	Difference	2,77%	1,35%	-1,06%	1,87%
Class 3	Test	2,70	10,57	3,19	11,34
	Model	2,87	11,88	3,30	13,30
	Difference	6,30%	12,39%	3,45%	17,28%
Rejected	Test	1,60	9,67	1,96	8,91

Conclusions

In conclusion, 400 board specimens from fir and black pine species were visually graded according to TS 1265 (2012) and stress wave method was applied for nondestructive tests.

Then, boards were tested under flatwise bending and load-deflection relationships were given detailly for each grade. After the statistical analysis, the mean values of MOR and MOE differed to three visual classes and rejected at a p<0,05 significance level.

Hence, high correlations between modulus of rupture and knot ratio indicated that limiting parameters of visual grading standard were suitable for boards.

To optimize visual grading, KDR calculation method in the existing standard could be improved especially for edge knots. Further more, the mechanical properties of boards under bending were not affected statistically by the angle between the flat surface of the samples and annual rings.

After comparing the visual grading and the stress wave method, it was discovered that visual grading was more reliant to sort board specimens into classes since the difference in the mean values of MOE between visual grades were more remarkable than the mean values of MOE_d. For the determination of dynamic modulus of elasticity, however, the usage of the defect-free density performed better than whole specimen's density specially to detect rejected samples. Overall, flexural stiffness obtained by destructive tests were 14,6 % for fir 10,9 % for black pine higher than nondestructive test results except for the rejected samples. The difference could be attributed to the small length of tested specimens and the transverse shear effects in the calculation of the global modulus of elasticity as stimulated by the latest version of CEN EN 408 (2012a)

The strength classes of boards were determined using destructive test results according to CEN EN 338 (2016b) with the required adjustments. The strength class assignments using flatwise bending were presented only for demonstration which should be considered carefully.

Since the specimens were taken from one region Bolu for fir and Balıkesir for black pine, no adjustment factors for the sampling were applied. Higher resistances were found for black pine boards in flatwise bending tests compared to edgewise bending classes defined in CEN EN

1912 (2012b). However, same resistances are found for fir boards in class 1 and class 3 except for class 2 with a small decrease. Therefore, more tests using flatwise bending are required to apply for the standardized system as boards used in engineered wood products are stressed in flatwise.

Lastly, the failure mode of boards under bending was observed by the rupture of timber fibers parallel-to-grain due to high tensile stresses for both species. With the proposal of a simplified nonlinear material model, experimental and numerical model results were found in good agreement in terms of bending strength and deformation capacity especially for class 1 and class 2 to model boards in structural applications. For class 3, the usage of linear material models should be appealed to be safer and more conservative in terms of the deformation capacity. For future studies, an experimental campaign is planned to produce and test cross-laminated timber panels by using the structural timber boards from Turkish fir and black pine.

Authorship contributions

F.K.: Conceptualization, data curation, formal analysis, investigation, methodology, resources, software, validation, visualization, writing – original draft, writing – review & editing. Ö.A.Ş.: Data curation, formal analysis, investigation, methodology, software, validation, visualization, writing – original draft, writing – review & editing. T.D.: Conceptualization, funding acquisition, methodology, project administration, resources, supervision, validation, writing - review & editing.

References:
ASTM. 2018. Standard practice for establishing allowable properties for structural glued laminated timber (Glulam). D3737. American Society for Testing and Methods, West Conshohosken.
Arriaga, F.; Osuna-Sequera, C.; Bobadilla, I.; Esteban, M. 2022. Prediction of the mechanical properties of timber members in existing structures using the dynamic modulus of elasticity and visual grading parameters. *Construction and Building Materials* 322: e126512.https://doi.org/10.1016/j.conbuildmat.2022.126512

Barriola, M.; Aira, J.; Villanueva, J. 2021. Analytical models of the mechanical properties of Japanese larch (*Larix kaempferi* (Lamb.) Carr.) based on non-destructive testing and visual grading parameters. *Wood Material Science & Engineering* 16(2): 94-101. https://doi.org/10.1080/17480272.2019.1626481

Barriola, M.J.; Aira, J.R.; Lafuente, E. 2020. Visual grading criteria for Japanese larch (Larix kaempferi) structural timber from Spain. *Journal of Forestry Research* 31(6): 2605-2614.https://doi.org/10.1007/s11676-019-01025-5

Berg, S.; Turesson, J.; Ekevad, M.; Huber, J.A.2019. Finite element analysis of bending stiffness for cross-laminated timber with varying board width. *Wood Material Science & Engineering* 14(6): 392-403. https://doi.org/10.1080/17480272.2019.1587506

BS. 2017. Visual strength grading of softwood. Specification. BS. 4978. 2007+A2. 2017. London. https://bsol.bsigroup.com/Bibliographic

Bucur, V. 2006. *Acoustics of Wood*. Springer Science & Business Media.

Burawska-Kupniewska, I.; Krzosek, S.; Mańkowski, P.; Grześkiewicz, M. 2020. Quality and Bending Properties of Scots Pine (*Pinus sylvestris* L.) Sawn Timber. *Forests* 11(11): e1200. https://doi.org/10.3390/f11111200

CSI. 2000. SAP 2000. Integrated finite element analysis and design of structures. Ver. 21. Berkeley, CA. https://www.csiamerica.com/products/sap2000

Crovella, P.; Smith, W.; Bartczak, J. 2019. Experimental verification of shear analogy approach to predict bending stiffness for softwood and hardwood cross-laminated timber panels. *Construction and Building Materials* 229: e116895.https://doi.org/10.1016/j.conbuildmat.2019.116895

DIN. 2012. Strength grading of wood – Part 1: Coniferous sawn timber DIN 4074-1. Berlin. https://www.din.de/en/getting-involved/standards-committees/nhm/publications/wdc-beuth:din21:151716980

Divós, F.; Kiss, F.S. 2010. Strength Grading of Structural Lumber by Portable Lumber Grading - effect of knots. The Future of Quality Control for Wood & Wood Products. 4-7th May 2010. Edinburgh, The Final Conference of COST Action (Volume 53).

Esteban, L.G.; Fernández, F.G.; de Palacios, P. 2009. MOE prediction in Abies pinsapo Boiss. timber: Application of an artificial neural network using non-destructive testing. *Computers & Structures* 87(21-22): 1360-1365. https://doi.org/10.1016/j.compstruc.2009.08.010

ECS. 2002. Moisture content of a piece of sawn timber - Part 1: Determination by oven dry method. EN 13183-1:2002. CEN: Brussels, Belgium.

ECS. 2012a. Timber structures - Structural timber and glued laminated timber - Determination of some physical and mechanical properties. EN 408:2010+A1:2012. CEN Brussels, Belgium.

ECS. 2012b. Structural timber - Strenght classes - Assignment of visual grades and species. EN 1912:2012. CEN: Brussels, Belgium.

ECS. 2013. Timber structures - Glued laminated timber and glued solid timber - Requirements. EN 14080:2013. CEN: Brussels, Belgium.

ECS. 2015. Timber structures - Cross laminated timber – Requirements. EN 16351:2015. CEN: Brussels, Belgium.

ECS. 2016a. Timber structures - Calculation and verification of characteristic values. EN 14358:2016. CEN: Brussels, Belgium.

ECS. 2016b. Structural Timber - Strength classes. EN 338:2016. CEN: Brussels, Belgium.

ECS. 2018a. Structural timber - Determination of characteristic values of mechanical properties and density. EN 384:2016+A1:2018. CEN: Brussels, Belgium. https://standards.cencenelec.eu/dyn/www/f?p=CEN:110:0:::FSP_PROJECT,FSP_ORG_ID:68122,6106&cs=112A171326697217D743EBDC1D81E1A0D

ECS. 2018b. Round and sawn timber - method and measurement. Part 3: Features and biological degradations. EN 1309-3:2018. CEN: Brussels, Belgium.

ECS. 2019. Round and Sawn Timber. Terminology. EN 884.2019. CEN: Brussels, Belgium.

Frese, M.; Enders-Comberg, M.; Blaß, H.J.; Glos, P. 2012. Compressive strength of spruce glulam. *European Journal of Wood and Wood Products* 70(6): 801-809.https://doi.org/10.1007/s00107-012-0623-x

Görgün, H.V.; Dündar, T. 2018. Strength grading of turkish black pine structural timber by visual evaluation and nondestructive testing. *Maderas. Ciencia y Tecnología* 20(1): 57-66. https://www.scielo.cl/scielo.php?script=sci_arttext&pid=S0718-221X2018000100057&lng=es&nrm=iso&tlng=en

Guntekin, E.; Bulbul, Z. 2014. Determination of bending properties for Black pine (*Pinus nigra* A.) lumber using stress wave method. *Düzce Üniversitesi Orman Fakültesi Ormancılık Dergisi* 10(2): 11-17. http:// https://www.cabdirect.org/cabdirect/abstract/20153184545

Guntekin, E.; Emiroglu, Z.G.; Yilmaz, T. 2013. Prediction of bending properties for turkish red Pine (*Pinus brutia* Ten.) lumber using stress wave method. *BioResources* 8(1): 231-237. https://bioresources.cnr.ncsu.edu/resources/prediction-of-bending-properties-for-turkish-red-pine-pinus-brutia-ten-lumber-using-stress-wave-method/

Kandler, G.; Lukacevic, M.; Füssl, J. 2018. Experimental study on glued laminated timber beams with well-known knot morphology. *European Journal of Wood and Wood Products* 76(5): 1435-1452. https://doi.org/10.1007/s00107-018-1328-6

Kohler, J.; Brandner, R.; Thiel, A.B.; Schickhofer, G. 2013. Probabilistic characterisation of the length effect for parallel to the grain tensile strength of Central European spruce. *Engineering Structures* 56: 691-697. http://dx.doi.org/10.1016/j.engstruct.2013.05.048

Köhler, J.; Sørensen, J.D.; Faber, M.H. 2007. Probabilistic modeling of timber structures. *Structural Safety* 29(4): 255-267. https://doi.org/10.1016/j.strusafe.2006.07.007

Mitsuhashi, K.; Poussa, M.; Puttonen, J. 2008. Method for predicting tension capacity of sawn timber considering slope of grain around knots. *Journal of Wood Science* 54(3): 189-195.https://doi.org/10.1007/s10086-007-0941-5

Mvolo, C.S.; Stewart, J.D.; Koubaa, A. 2021. Comparison between static modulus of elasticity, non-destructive testing moduli of elasticity and stress-wave speed in white spruce and lodgepole pine wood. *Wood Material Science & Engineering* 17(5): 345-355. https://doi.org/10.1080/17480272.2021.1871949

Navaratnam, S.; Christopher, P.B.; Ngo, T.; Le, T.V. 2020. Bending and shear performance of Australian Radiata pine cross-laminated timber. *Construction and Building Materials* 232: e117215.https://doi.org/10.1016/j.conbuildmat.2019.117215

Nwokoye, D. 1972. Investigation into an ultimate beam theory for rectangular timber beams-solid and laminated. *Timber Res Develop Ass Res Rep E/rr 34*

OGM. 2021. T.C. Tarım ve Orman Bakanlığı Orman Genel Müdürlüğü. https://www.ogm.gov.tr/tr

Olsson, A.; Oscarsson, J.; Serrano, E.; Källsner, B.; Johansson, M.; Enquist, B. 2013. Prediction of timber bending strength and in-member cross-sectional stiffness variation on the basis of local wood fibre orientation. *European Journal of Wood and Wood Products* 71(3): 319-333.https://doi.org/10.1007/s00107-013-0684-5

Pang, S.J.; Shim, K.B.; Kim, K.H. 2021. Effects of knot area ratio on the bending properties of cross-laminated timber made from Korean pine. *Wood Science and Technology* 55: 489-503.https://doi.org/10.1007/s00226-020-01255-5

Ross, R.J. 2015. Nondestructive evaluation of wood. General Technical Report. USDA Forest Service, Forest Products Laboratory. General Technical Report, FPL-GTR-238. 176 p.

Rais, A.; Bacher, M.; Khaloian-Sarnaghi, A.; Zeilhofer, M.; Kovryga, A.; Fontanini, F.; Hilmers, T.; Westermayr, M.; Jacobs, M.; Pretzsch H.; van de Kuilen, J. W. 2021. Local

3D fibre orientation for tensile strength prediction of European beech timber. *Construction and Building Materials* 279: e122527. https://doi.org/10.1016/j.conbuildmat.2021.122527

Sanabria, S.J.; Furrer, R.; Neuenschwander, J.; Niemz, P.; Sennhauser, U. 2011. Air-coupled ultrasound inspection of glued laminated timber. *Holzforschung.*65(3): 377-387. https://doi.org/10.1515/hf.2011.050

Stapel, P.; van de Kuilen, J.W. 2014. Influence of cross-section and knot assessment on the strength of visually graded Norway spruce. *European Journal of Wood and Wood Products* 72(2): 213-227. https://doi.org/10.1007/s00107-013-0771-7

TS. 2012. Sawn timber (Coniferous) - For building construction. TSE 1265. Ankara, Turkey.

UNI. 2010. Structural timber - Visual strength grading for structural timbers - Part 1: Terminology and measurements of features. UNI 11035-1. Milano, Italy.

UNE. 2011. Visual grading for structural sawn timber. Coniferous timber. UNE. 56544. Madrid, Spain.

Van Duong, D.; Matsumura, J. 2018. Within-stem variations in mechanical properties of *Melia azedarach* planted in northern Vietnam. *Journal of Wood Science* 64(4): 329-337. https://doi.org/10.1007/s10086-018-1725-9

Van Duong, D.; Ridley-Ellis, D. 2021. Estimating mechanical properties of clear wood from ten-year-old Melia azedarach trees using the stress wave method. *European Journal of Wood and Wood Products* 79(4): 941-949. https://doi.org/10.1007/s00107-021-01664-8

Vega, A.; González, L.; Fernández, I.; González, P. 2019. Grading and mechanical characterization of small-diameter round chestnut (*Castanea sativa* Mill.) timber from thinning operations. *Wood Material Science & Engineering* 14(2): 81-87. https://doi.org/10.1080/17480272.2017.1387174